Characterization of the Atmospheric State above the SGP Using Raman Lidar and AERI/GOES Measurements

R. A. Ferrare
National Aeronautics and Space Administration
Langley Research Center
Hampton, Virginia

D. D. Turner
Pacific Northwest National Laboratory
Richland, Washington

T. P. Tooman
Sandia National Laboratories
Livermore, California

L. A. Heilman
Science Applications International Corporation
National Aeronautics and Space Administration
Langley Research Center
Hampton, Virginia

O. Dubovik
Science Systems and Applications, Inc.
National Aeronautics and Space Administration
Goddard Space Flight Center
Greenbelt, Maryland

W. F. Feltz
University of Wisconsin
Madison, Wisconsin

R. N. Halthore
Brookhaven National Laboratory
Upton, New York

Introduction

We have developed and implemented automated algorithms to retrieve profiles of water vapor mixing ratio, aerosol backscattering, and aerosol extinction from Southern Great Plains (SGP) Cloud and Radiation Testbed (CART) Raman lidar data acquired during both daytime and nighttime operations. This Raman lidar system is unique in that it is a turnkey, automated system designed for unattended, around-the-clock profiling of water vapor and aerosols (Goldsmith et al. 1998). These Raman lidar profiles are important for determining the clear-sky radiative flux, as well as for validating the retrieval algorithms associated with satellite sensors. Accurate, high spatial and temporal resolution profiles of water vapor are also required for assimilation into mesoscale models to improve weather forecasts.

We have also developed and implemented routines to simultaneously retrieve profiles of relative humidity. These routines utilize the water vapor mixing ratio profiles derived from the Raman lidar measurements together with temperature profiles derived from a physical retrieval algorithm that uses data from a collocated atmospheric emitted radiance interferometer (AERI) and the Geostationary Operational Environmental Satellite (GOES) (Feltz et al. 1998; Turner et al. 2000). These aerosol and water vapor profiles (Raman lidar) and temperature profiles (AERI+GOES) have been combined into a single product that takes advantage of both active and passive remote sensors to characterize the clear-sky atmospheric state above the CART site.

Instrumentation

The CART Raman lidar (CARL) uses a tripled Nd:YAG laser, operating at 30 Hz with 350 millijoule to 400 millijoule pulses to transmit light at 355 nm. A 61-cm-diameter telescope collects the light back-scattered by molecules and aerosols at the laser wavelength and the Raman scattered light from water vapor (408 nm) and nitrogen (387 nm) molecules. These signals are detected by photomultiplier tubes and recorded using photon counting with a vertical resolution of 39 m. A beam expander reduces the laser beam divergence to 0.1 mrad, thereby permitting the use of a narrow (0.3 mrad) as well as a wide (2 mrad) field of view. The narrow field of view, coupled with the use of narrowband (~0.4 nm band-pass) filters, reduces the background skylight and, therefore, increases the maximum range of the aerosol and water vapor profiles measured during daytime operations.

Water vapor mixing ratio profiles are computed using the ratio of the Raman water vapor signal to the Raman nitrogen signal. Relative humidity profiles are computed using these water vapor mixing ratio profiles and the temperature profiles from the AERI+GOES temperature retrievals. The water vapor mixing ratio profiles are integrated with altitude to derive precipitable water vapor (PWV). The CARL water vapor mixing ratio profiles and PWV retrievals are calibrated using the coincident nighttime measurements of PWV from the microwave radiometer (MWR) (Turner and Goldsmith 1999). The CARL water vapor calibration factor derived in this manner over a period of 9 months has a standard deviation of approximately 4% (Turner et al. 2000).

The lidar water vapor mixing ratio profiles were compared with water vapor profiles measured by radiosondes equipped with Vaisala RS-80 H-humicap sensors. Figure 1a shows the mean ratio between CARL and radiosonde water vapor mixing ratio profiles. The unscaled radiosonde profiles are drier than the CARL profiles by about 3% to 5%; scaling the radiosonde profiles by the MWR PWV reduces this bias to about 1% to 2%. This scaling also reduces the differences between measured and modeled longwave radiances (Turner et al. 1998). Figure 1b shows that the temperature differences between the AERI+GOES retrievals and the radiosondes are generally less than 1 K.

Profiles of aerosol scattering ratio, which is the ratio of aerosol+molecular scattering to molecular scattering, are derived using the Raman nitrogen signal and the signal detected at the laser wavelength. Aerosol volume backscattering cross-section profiles are then computed using the aerosol scattering ratio and molecular scattering cross-section profiles derived from atmospheric density data. These density profiles are computed using coincident pressure and temperature profiles derived from radiances measured by the ground-based AERI instrument and by the GOES satellite. Aerosol extinction cross-section profiles are computed from the derivative of the logarithm of the Raman nitrogen signal with respect to range. The aerosol backscattering and extinction profiles derived in this manner are then used to measure profiles of the aerosol extinction/backscattering ratio. Aerosol optical thicknesses are derived by integration of the aerosol extinction profiles with altitude. Ferrare et al. (1998) provide additional information regarding these methods.

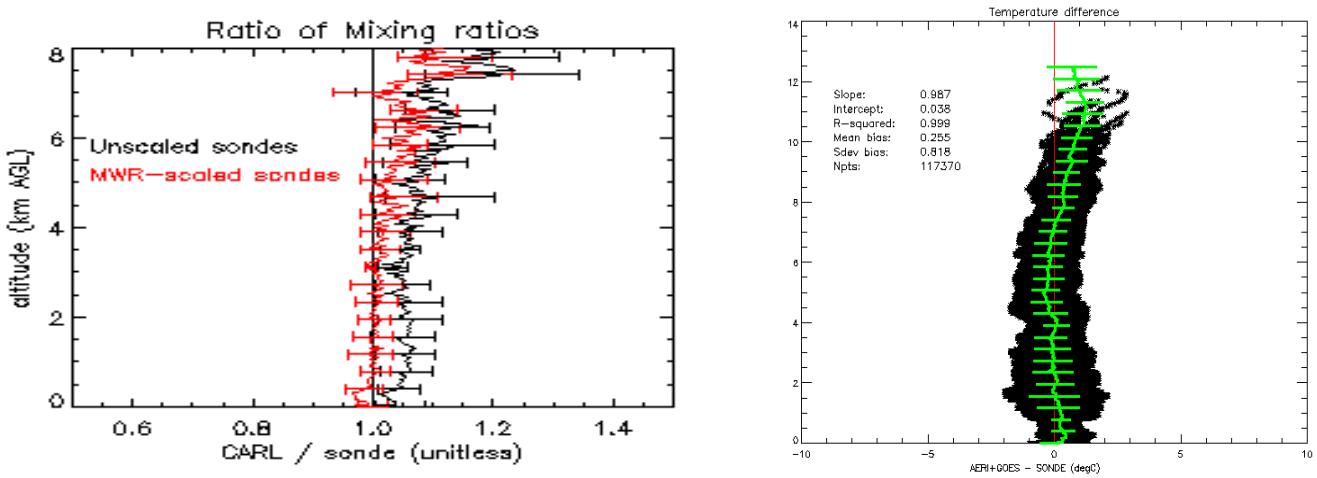

(a) (b)

Figure 1. (a) Ratio between CARL and radiosonde unscaled (black) and scaled (red) water vapor mixing ratio profiles acquired from April 1998 through October 1999. (b) Difference between AERI+GOES and radiosonde temperature profiles over this same period.

Measurements

In this paper, we discuss aerosol extinction, water vapor, and relative humidity profiles computed using the automated algorithms for Raman lidar data acquired between April 1, 1998, and April 30, 1999. During this period, CARL operated nearly 50% of the time, with electrical power interruptions responsible for most of the down time.

The high resolution Raman lidar water vapor measurements and AERI temperature measurements provide a much more detailed representation of the atmospheric state than can be achieved using radiosondes alone. These measurements depict in great detail the rapid atmospheric changes associated with the passages of dry lines, cold fronts, and other synoptic features over the SGP site. Figure 2 shows water vapor mixing ratio, relative humidity, temperature, and aerosol extinction profiles derived from CARL and AERI data acquired on April 15, 1998. These images show the passage of a cold front between 0900 Universal Time Coordinates (UTC) and 1100 UTC. Note the rapid decrease in water vapor mixing ratio and temperature after the front passed over the site. An increase in aerosol extinction associated with hygroscopic aerosol growth can be seen between 0800 UTC and 1000 UTC just prior to the frontal passage when the relative humidity increased above 70%. Turner et al. (2000) give a more complete description of this event and how the CARL and AERI data complement each other in characterizing the atmospheric state.

We have begun using the CARL aerosol data to characterize aerosol extinction, backscattering, and optical thickness over the SGP site. Average aerosol extinction profiles were computed as a function of optical thickness to characterize the vertical distribution of aerosols. Figure 3 shows the average aerosol extinction profiles as a function of AOT as well as the distribution of AOT during each season. These profiles show a large season variability in AOT as well as how the vertical variability varies with season.

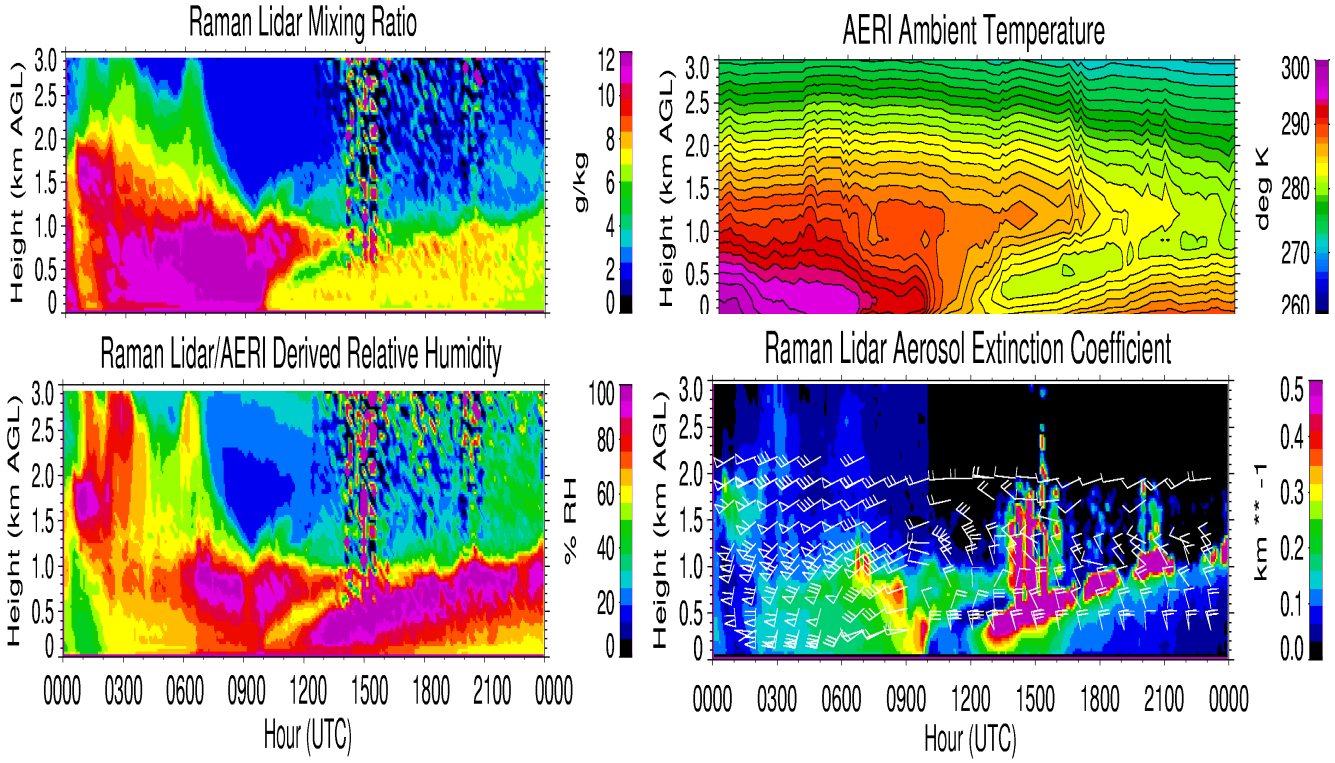

Figure 2. Profiles of water vapor mixing ratio (top left), relative humidity (bottom left), temperature (top right), and aerosol extinction (bottom right) measured over the SGP site on April 15, 1998, showing the passage of a cold front. Water vapor mixing ratio and aerosol extinction were derived from CARL, temperature from AERI, and relative humidity from both sensors. The vertical stripes that appear in the water vapor, relative humidity, and aerosol extinction images between 1400 UTC and 1600 UTC are due to clouds.

Aerosol extinction profiles acquired during May and August-September 1998 show episodes when high aerosol extinction was measured throughout several kilometers in the lower troposphere over several days. The Raman lidar aerosol extinction profiles derived during May 13 through May 21 were most likely associated with the smoke from fires in Central America since observations by several satellite sensors and trajectory analyses indicated that smoke produced by these fires traveled over northern Oklahoma (Peppler et al. 1999).

We have also begun using these lidar aerosol and water vapor profiles to investigate lidar aerosol extinction/backscattering ratio (S_a), and the relationships among water vapor mixing ratio, relative humidity, aerosol extinction, and aerosol extinction/backscatter ratio for hygroscopic aerosols. CARL data often show that the aerosol extinction increased significantly when the relative humidity increased above 60% to 70% near the top of the boundary layer. Figure 4 shows how aerosol extinction measured near the top of the daytime boundary layer varied with relative humidity as deduced from the CARL measurements. This behavior is somewhat similar to that derived for aerosol scattering using ground-based nephelometer measurements of aerosol scattering.

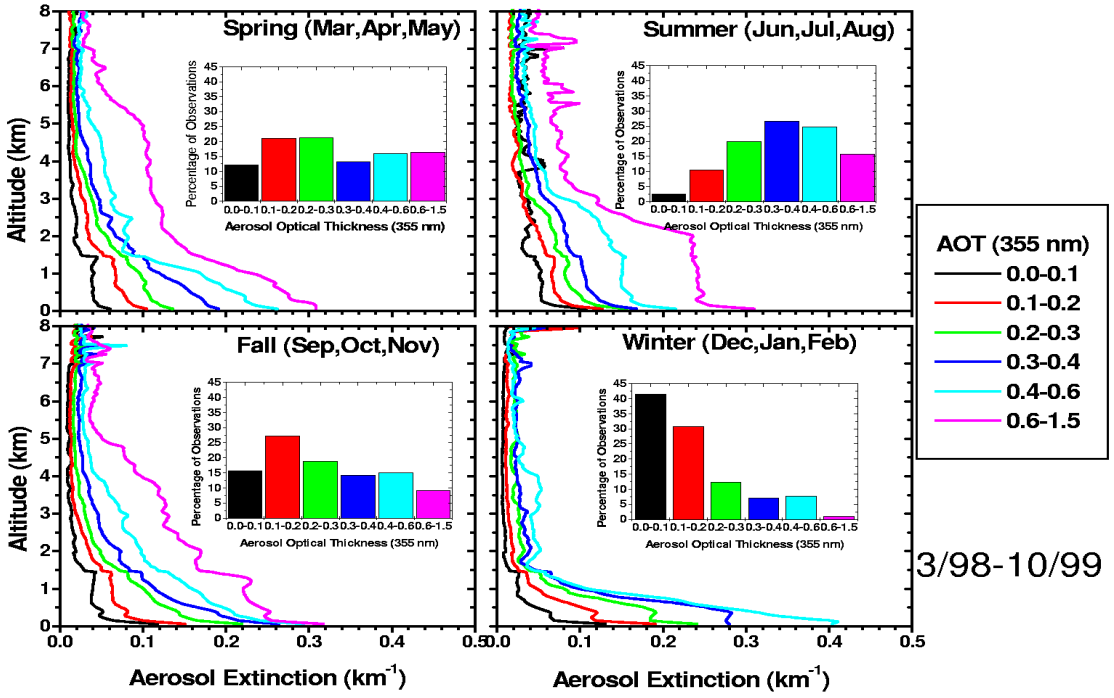

Figure 3. Distribution of aerosol optical thickness and average aerosol extinction profiles for each season using CARL data acquired between March 1998 and October 1999.

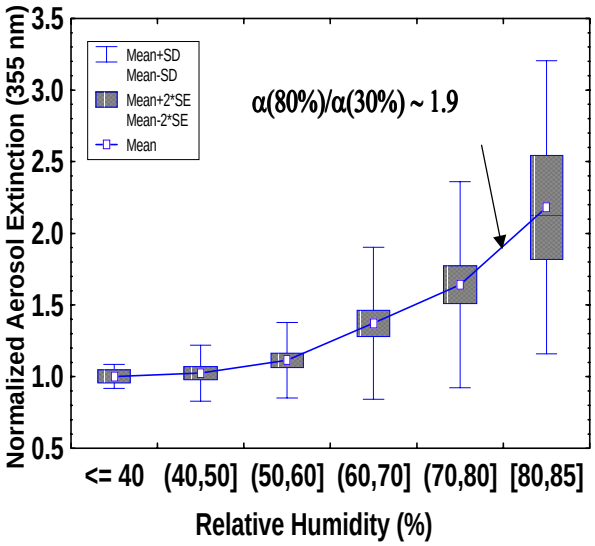

Figure 4. Aerosol extinction as a function of relative humidity near the top of the daytime boundary layer as derived from CARL measurements.

The aerosol extinction/backscattering ratio S_a, which we also derive from the CARL measurements, often indicates variations in either the size and/or composition of the aerosols. Figure 5a shows how S_a varies with changes in the aerosol Angstrom exponent. As this exponent decreases from -1 to -2, aerosol particle sizes decrease and S_a tends to increase. Aerosol particle sizes and refractive indices were derived using the procedure developed by Dubovik et al. (1999), which uses measurements of aerosol optical thickness and almucantar sky radiance acquired by a ground-based Cimel sun photometer. Figure 5b shows that S_a increases as the aerosol fine mode volume increases so that CARL measurements of S_a may indicate changes in the aerosol size distribution. Moreover, the CARL retrievals of S_a as a function of altitude show large (>20%) variations in S_a occur 25% of the time. This information is important because passive retrievals of aerosol size and composition based on ground- or space-based measurements provide only column-averaged values.

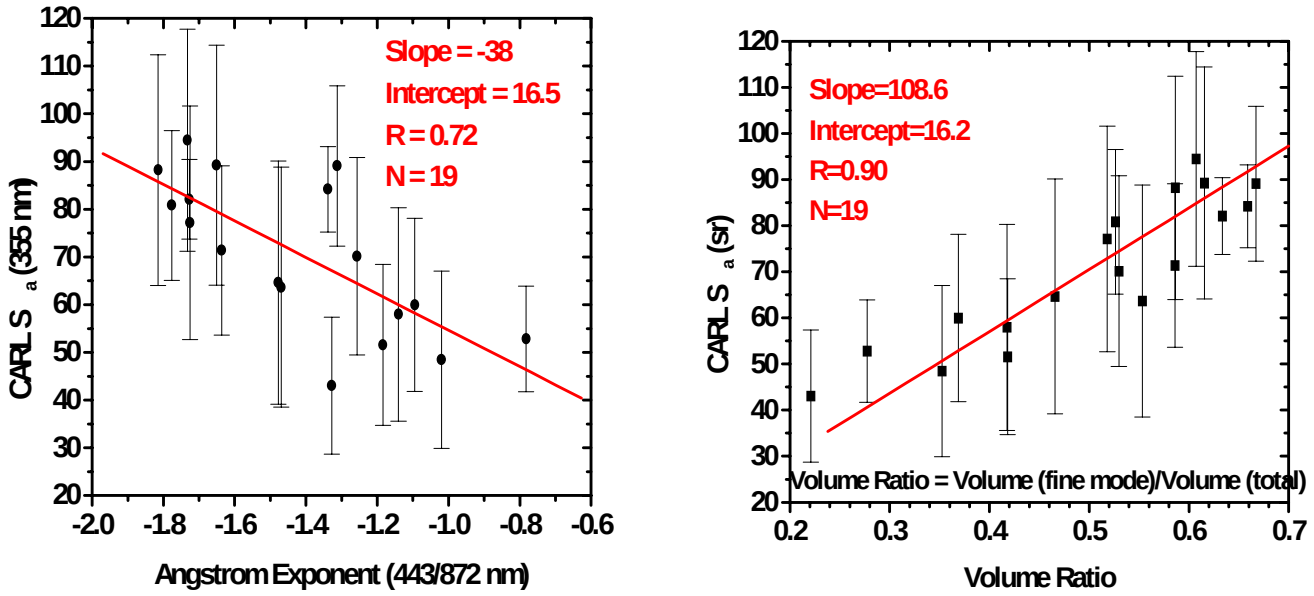

(a) (b)

Figure 5. (a) Variation of the aerosol extinction/backscattering ratio S_a derived from CARL data with the aerosol Angstrom exponent derived from Cimel Sun photometer data. (b) Variation in S_a as function of the ratio between the aerosol fine mode and total aerosol volumes.

Summary

We have implemented algorithms to compute aerosol extinction and relative humidity profiles using CART Raman lidar data and AERI+GOES temperature retrievals. Together with Raman lidar water vapor mixing ratio, cloud mask, and depolarization retrievals, these aerosol and relative humidity profiles form a suite of products that are retrieved using automated remote sensing instruments and can be used to characterize the clear-sky state over the SGP site. We are using these Raman lidar aerosol and water vapor measurements to investigate the relationships among water vapor and aerosols.

Acknowledgments

SGP CART Raman lidar, Cimel sun photometer, and AERI data were obtained from the Atmospheric Radiation Measurement (ARM) Program sponsored by the U.S. Department of Energy (DOE), Office of Energy Research, Office of Health and Environmental Research, Environmental Sciences Division. The Cimel sun photometer is also part of AERONET, a network of sun photometers managed by B. N. Holben, National Aeronautics and Space Administration (NASA)-Goddard Space Flight Center (GSFC). Funding for this work was provided by the NASA-Earth Observing System Validation and DOE ARM Programs.

Corresponding Author

R. A. Ferrare, NASA Langley Research Center, MS 401A, Hampton, VA 23681, (757) 864-9443, r.ferrare@larc.nasa.gov

References

Dubovik, O., M. D. King, B. N. Holben, Y. J. Kaufman, A. Smirnov, T. F. Eck, and I. Slutsker, 1999: A flexible inversion algorithm for retrieval of aerosol optical properties from sun and sky radiance measurements. *J. Geophys. Res.* Submitted.

Feltz, W. F., W. L. Smith, R. O. Knuteson, H. E. Revercomb, H. M. Woolf, and H. B. Howell, 1998: Meteorological applications of temperature and water vapor retrievals from the ground-based atmospheric emitted radiance interferometer (AERI). *J. Appl. Meteor.*, **37**, 857-875.

Ferrare, R. A., S. H. Melfi, D. N. Whiteman, K. D. Evans, and R. Leifer, 1998: Raman lidar measurements of aerosol extinction and backscattering: Methods and comparisons. *J. Geophys Res.*, **103**, 19,663-19,672.

Goldsmith, J. E. M., F. H. Blair, S. E. Bisson, and D. D. Turner, 1998: Turn-key Raman lidar for profiling atmospheric water vapor, clouds, and aerosols. *Appl. Opt*, **37**, 4979-4990.

Peppler, R. A., L. Ashford, C. P. Bahrmann, J. C. Barnard, R. A. Ferrare, R. N. Halthore, N. S. Laulainen, J. A. Ogren, P. J. Sheridan, M. E. Splitt, and D. D. Turner, 1999: Identification and analysis of the 1998 Central American smoke event at the ARM SGP CART site. *Proceedings of the Ninth Atmospheric Radiation Measurement (ARM) Science Team Meeting,* U.S. Department of Energy, Washington, D.C. Available URL: http://www.arm.gov/docs/documents/technical/conf_9903/peppler-99.pdf

Turner, D. D., T. R. Shippert, P. D. Brown, S. A. Clough, R. O. Knuteson, H. E. Revercomb, and W. L. Smith, 1998: Long-term analyses of observed and line-by-line calculations of longwave surface spectral radiance and the effect of scaling the water vapor profile. In *Proceedings of the Eighth Atmospheric Radiation Measurement (ARM) Science Team Meeting*, DOE/ER-0738, pp. 773-776. U.S. Department of Energy, Washington, D.C. Available URL: http://www.arm.gov/docs/documents/technical/conf_9803/turner-98.pdf

Turner, D. D., and J. E. M. Goldsmith, 1999: 24-Hour Raman lidar measurements during the Atmospheric Radiation Measurement Program's 1996 and 1997 Water Vapor Intensive Observation Periods. *J. Atmos. Oceanic Technol.*, **16**, 1062-1076.

Turner, D. D., W. F. Feltz, and R. A. Ferrare, 2000: Continuous water profiles from operational ground-based active and passive remote sensors. *Bull. Amer. Meteor. Soc.* In press.